AGU PUBLICATIONS

JGR

Journal of Geophysical Research: Atmospheres

RESEARCH ARTICLE
10.1002/2016JD025555

Key Points:
- The slope of amount effect in the tropics reduces with reduction in modeled deep convective precipitation
- Increases in large-scale/shallow convective precipitation partially offset the reduction in the slope of amount effect
- The δD_{precip} values are improved in certain regions in tropics with reduced deep convection

Supporting Information:
- Supporting Information S1

Correspondence to:
T. Tharammal,
thejna@caos.iisc.ernet.in

Citation:
Tharammal, T., G. Bala, and D. Noone (2017), Impact of deep convection on the isotopic amount effect in tropical precipitation, *J. Geophys. Res. Atmos.*, *122*, doi:10.1002/2016JD025555.

Received 21 JUN 2016
Accepted 18 JAN 2017
Accepted article online 22 JAN 2017

Impact of deep convection on the isotopic amount effect in tropical precipitation

Thejna Tharammal[1], Govindasamy Bala[2], and David Noone[3]

[1]Divecha Center for Climate Change, Indian Institute of Science, Bangalore, India, [2]Divecha Center for Climate Change, Center for Atmospheric and Oceanic Sciences and Interdisciplinary Center for Water Research, Indian Institute of Science, Bangalore, India, [3]College of Earth, Ocean and Atmospheric Sciences, Oregon State University, Corvallis, Oregon, USA

Abstract The empirical "amount effect" observed in the distribution of stable water isotope ratios in tropical precipitation is used in several studies to reconstruct past precipitation. Recent observations suggest the importance of large-scale organized convection systems on amount effect. With a series of experiments with Community Atmospheric Model version 3.0 with water isotope tracers, we quantify the sensitivity of amount effect to changes in modeled deep convection. The magnitude of the regression slope between long-term monthly precipitation amount and isotope ratios in precipitation over tropical ocean reduces by more than 20% with a reduction in mean deep convective precipitation by about 60%, indicating a decline in fractionation efficiency. Reduced condensation in deep convective updrafts results in enrichment of lower level vapor with heavier isotope that causes enrichment in total precipitation. However, consequent increases in stratiform and shallow convective precipitation partially offset the reduction in the slope of amount effect. The net result is a reduced slope of amount effect in tropical regions except the tropical western Pacific, where the effects of enhanced large-scale ascent and increased stratiform precipitation prevail over the influence of reduced deep convection. We also find that the isotope ratios in precipitation are improved over certain regions in the tropics with reduced deep convection, showing that analyses of isotope ratios in precipitation and water vapor are powerful tools to improve precipitation processes in convective parameterization schemes in climate models. Further, our study suggests that the precipitation types over a region can alter the fractionation efficiency of isotopes with implications for the reconstructions of past precipitation.

1. Introduction

Stable isotopic composition of meteoric water is a hydrological tracer and is used as a climate proxy to reconstruct past temperature and precipitation. Due to the differences in the saturation vapor pressures of heavier and lighter isotopes of water, a temperature-dependent fractionation occurs during the phase transitions during condensation and evaporation of the water molecule. During evaporation, lighter molecule is evaporated preferentially, and resultant vapor is depleted in heavy isotopes with respect to the liquid source. During condensation, the heavier molecule preferentially condenses, causing the remaining vapor to be further depleted of heavier isotopes. This leads to the observed variability in ratios of heavy to light isotopes (denoted by delta, δ, in units of per mil [‰]) in the global hydrological cycle. The water isotope ratios in precipitation in the higher latitudes show a strong positive correlation with the local surface temperature (temperature effect [*Dansgaard*, 1964]), and using this relationship, deep ice core oxygen isotope records from Greenland and Antarctica are used to interpret the past temperature variability [*Johnsen et al*., 1972; *Lorius et al*., 1985; *Stenni et al*., 2004].

In the tropics, the empirical "amount effect," introduced by *Dansgaard* [1964]—the anticorrelation between the monthly mean isotope ratio of precipitation and total amount of precipitation—is often used to decipher the past precipitation from the climate archives. For example, making use of the amount effect, climate proxies such as the hydrogen isotopic ratio of the plant wax compounds (δD_{wax}) from the sedimentary cores [e.g., *Schefuß et al*., 2005, 2011; *Tierney et al*., 2011; *Collins et al*., 2011, 2013; *Contreras-Rosales et al*., 2014; *Niedermeyer et al*., 2016] and the oxygen isotope archives from the cave stalagmites from low latitudes [e.g., *Dykoski et al*., 2005; *Pausata et al*., 2011] are used to interpret the water isotopic composition of the past precipitation, hence, to reconstruct the past precipitation variability. Similarly, amount effect is used for the reconstruction of past monsoon precipitation over Indian subcontinent using the oxygen isotope archives from both the cave stalagmites [*Burns et al*., 2002; *Yadava et al*., 2004; *Yadava and Ramesh*, 2005;

Laskar et al., 2013] and the isotope ratios derived from the tree rings [*Sano et al*., 2011; *Managave et al*., 2011]. These reconstructions use the present-day slope of amount effect as the transfer function, obtained from the regression analysis between the total precipitation and the isotopic ratio of precipitation from the nearby climate monitoring stations [e.g., *Yadava and Ramesh*, 2005], or a single universal slope of the relationship derived from a comprehensive range of tropical climate monitoring stations [e.g., *Niedermeyer et al*., 2016].

Several studies using observational data [e.g., *Kurita*, 2013] and climate models equipped with tracers for water isotope ratios [*Vuille et al*., 2003, 2005; *Bony et al*., 2008; *Risi et al*., 2008, 2010a, 2010b, 2012; *Lee and Fung*, 2008; *Tindall et al*., 2009] have attempted to quantify the present-day amount effect and to study the physical mechanism behind the amount effect. These studies explain amount effect based on (i) the increased condensation and rainout with heavy precipitation [*Vuille et al*., 2003]; (ii) reevaporation of precipitation and enhanced recycling of this isotopically depleted vapor in unsaturated downdrafts during intense convection [*Risi et al*., 2008]; (iii) drop-size-dependent partial equilibration of raindrops below the cloud base [*Lee and Fung*, 2008]; (iv) the dependence of isotope ratios of precipitation on the converged vapor, with the increased moisture convergence during the convective events, than on the vapor from the local evaporation [*Lee et al*., 2007; *Moore et al*., 2014]; and (v) increased rain amount and reduced proportion of reevaporation of falling raindrops in the convective systems [*Sutanto et al*., 2015]. Event-based observations from tropical stations over land [*Lekshmy et al*., 2014] and ocean [*Kurita*, 2013] find the dominant effect of the presence of organized convective systems on the amount effect. These two studies, in turn, attribute the amount effect on the postcondensational processes in the unsaturated downdrafts [*Lawrence et al*., 2004; *Risi et al*., 2008] through the environmental subsidence and mixing during the organized convective events. A recent observational study by *Aggarwal et al*. [2016] finds that the isotope ratios in tropical and midlatitude precipitation reflect the proportions of convective/stratiform rains.

These findings pave way to the question that whether the amount effect over the tropics, and over the monsoon regimes, is more related to changes in the total amount of precipitation or to the changes in the convective activity and to the types of precipitation at a region. Furthermore, we are motivated to examine the robustness of the transfer functions (the slope of the regression line between isotope ratios in precipitation and the amount of precipitation) used in the paleo-climate reconstructions.

In this study, we conduct a series of sensitivity experiments with National Center for Atmospheric Research Community Atmospheric Model version 3 [*Collins et al*., 2006; *Boville et al*., 2006; *Hack et al*., 2006] equipped with water isotope tracers (IsoCAM3.0) to investigate the relation between isotopic ratio of precipitation and deep convective precipitation. In order to modify the contribution of precipitation from the deep convective scheme we change the convective relaxation time scale, τ (the time taken to exhaust the convective available potential energy (CAPE) through convection) of the Zhang-McFarlane deep convection scheme [*Zhang and McFarlane*, 1995], in individual simulations adapting the method followed by *Lee et al*. [2009] and *Mishra and Srinivasan* [2010]. In addition, to identify the robustness of the inferred influence of convection on the isotope ratios in precipitation, we perform an idealized experiment designed to change the spatial pattern of precipitation by enhancing convection over land. The experiment is motivated by recent studies [e.g., *Bony et al*., 2013; *Chadwick et al*., 2014; *Modak et al*., 2016], which show that the convection over the land increases by the direct effect of increased CO_2 [*Dong et al*., 2009; *Bala et al*., 2010; *Cao et al*., 2012], as the continent warms faster relative to the ocean, thereby causing monsoon-type circulations over the globe.

2. Methods

The model simulations are performed with the Community Atmosphere Model (CAM), which is the atmospheric component of Community Climate System Model version 3.0 [*Collins et al*., 2006], and equipped with water isotope tracers in model physics based on *Noone and Simmonds* [2002] and *Noone* [2003] (hereafter IsoCAM3.0 [*Noone and Sturm*, 2010]). The Community Land Model serves as the land component of the model, which is coupled to the CAM. Isotope ratios over land surface are tracked by a simple bucket model [*Manabe*, 1969; *Deardorff*, 1977], derived from the scheme employed by *Noone and Simmonds* [2002]. IsoCAM3.0 was used for the simulation of distribution of isotope ratios in past climates [*Sturm et al*., 2010; *Tharammal et al*., 2013; *Contreras-Rosales et al*., 2014]. For our study, the model is

forced with prescribed sea surface temperature (SST)'s and sea ice fraction, with a spectral resolution of T_{85} (1.4° or ~155 km at the equator) in the horizontal and 26 levels in the vertical.

The model time step for all the simulations is set as the default 600 s for the T_{85} resolution.

In an earlier version of this model (CAM2.0 [*Lee et al*., 2009]), water isotope ratios have been shown to be sensitive to the strength of deep convective precipitation in the model which is parameterized in the model as the time scale, τ, over which CAPE is consumed by convection. Additionally, previous studies on parameter sensitivity in the *Zhang and McFarlane* [1995] convection scheme [*Scinocca and McFarlane*, 2004; *Jackson et al*., 2004; *Mishra and Srinivasan*, 2010; *Williamson*, 2013; *Yang et al*., 2013] show that the atmospheric deep convection is suppressed as the value of τ is increased. Therefore, we change the τ values from the default 1 h to 2, 4, 6, and 8 h in a series of experiments as in *Lee et al*. [2009] and *Mishra and Srinivasan* [2010]. A brief description of the model deep convective scheme is included in Text S1 in the supporting information. The simulation with the default value of τ as 1 h is called as Tau01 (control simulation), and those with τ values 2, 4, 6, and 8 h are termed as Tau02, Tau04, Tau06, and Tau08, respectively.

The isotope model traces the water isotopes as normal water in the model hydrology but undergo fractionation whenever a phase change occurs [*Merlivat and Nief*, 1967; *Majoube*, 1971; *Gedzelman and Arnold*, 1994; *Ciais and Jouzel*, 1994]. The enrichment of the ocean surface is fixed with a constant value of 0.5‰ for O^{18} and 4‰ for deuterium following *Hoffmann et al*. [1998] and *Craig and Gordon* [1965]. IsoCAM uses a semi-Lagrangian formulation for the water vapor and tracer transport [*Williamson and Olson*, 1994; *Williamson and Rasch*, 1994]. Some additional features of the isotope module in IsoCAM3.0 are described in Text S2.

The water isotopic composition is denoted by the delta (δ) value, and for a sample it is calculated with respect to the Vienna standard mean ocean water (VSMOW). For deuterium,

$$\delta D = \left(R_{\text{sample}}/R_{\text{VSMOW}} - 1\right) \times 1000$$

where R is the ratio of heavy to light isotope, D/H. Following the original work of *Dansgaard* [1964], the amount effect is calculated as the linear regression between long-term monthly means of the δD in precipitation (δD_{precip}) and tropical precipitation.

The model is run for a total of 22 years in the standard Atmospheric Model Intercomparison Project [*Gates et al*., 1999] configuration forced with observed sea surface temperature (SST) from the melded Hadley Centre Sea Ice and Sea Surface Temperature/Reynolds climatology for 1979–2001 [*Hurrell et al*., 2008], and the last 20 years of the simulations are analyzed for discussing the results. The orbital parameters are set at values corresponding to 1950 A.D.

Additionally, we conducted two experiments identical to the Tau series experiments, with the τ values set to 10 h and 12 h, termed as Tau10 and Tau12, respectively. We believe that a τ value of 12 h or more is likely unrealistic since the time interval between CAPE generation and dissipation is unlikely to be larger than half a day. While most of our discussion is confined to the experiments with τ values 1, 2, 4, 6, and 8 h, the longer list of seven Tau series experiments is used to estimate the τ value at which the agreement between isotopic ratios in precipitation simulated by the model and observations is a maximum. The results of these root-mean-square error (RMSE) estimates are given in section 3.4.

We conduct an additional experiment that is designed to evaluate the impact of enhanced convective activity over land on the amount effect. This is accomplished by quadrupling atmospheric CO_2 concentration in the experiment ($4\times CO_2$_RF) with the SSTs fixed. With prescribed SSTs the higher radiative forcing requires the land to warm and consequently enhances continental convection. The simulation is not intended to be a climate change experiment, and hence, the purpose is not to investigate the changes in isotope ratios in a warming climate. For this simulation, only the atmospheric CO_2 concentration is quadrupled with respect to the control value of 355 ppm, while the SST, sea ice, and other boundary conditions are kept the same as the control configuration. The model is run for 15 years, and the last 10 years are used for the analysis.

We investigate the responses in the tropical isotope ratios of the water vapor, convective updrafts, liquid condensate, and of the precipitation reaching the ground to the changes in deep convection in the model. A brief comparison of the simulated isotope distribution in tropical precipitation with the Global Network of Isotopes in Precipitation (GNIP) data [*International Atomic Energy Agency* (*IAEA*)/*Global Network of Isotopes in Precipitation* (*GNIP*), 2015] is also included in the results.

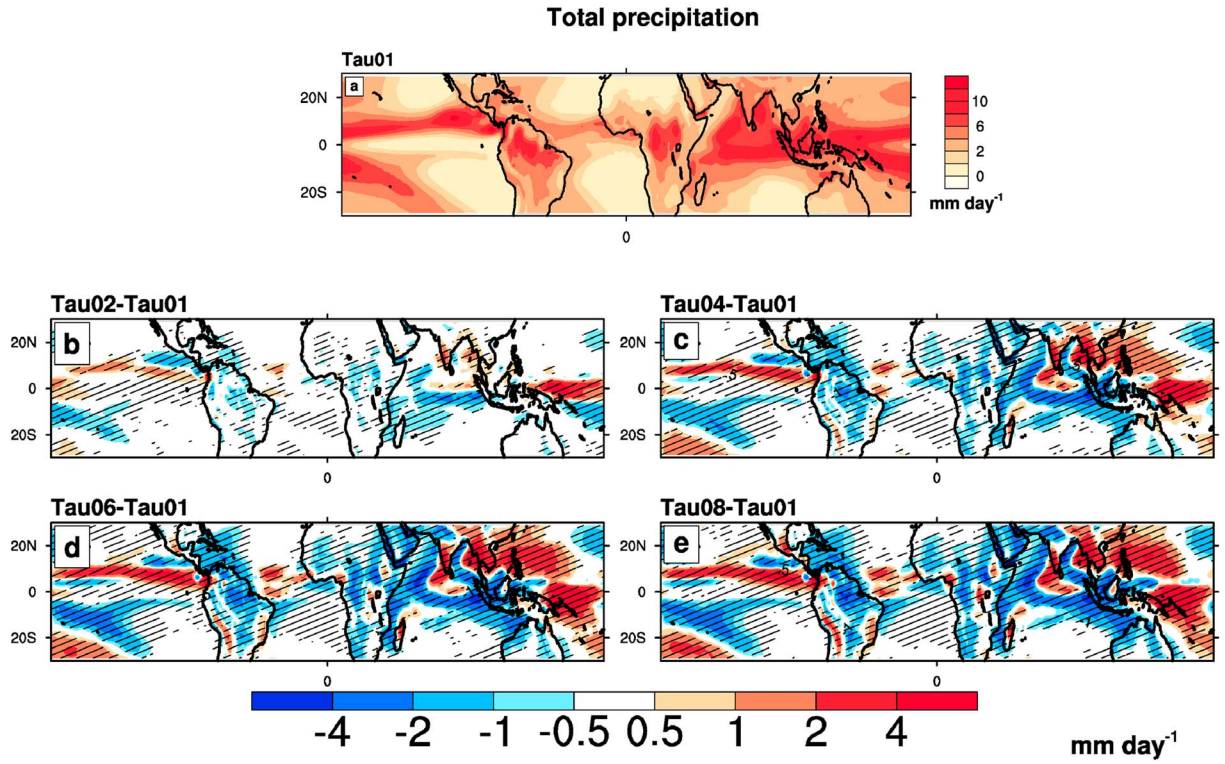

Figure 1. (a) Total precipitation in the control simulation (Tau01) in the tropics (m d^{-1}) and (b–e) the anomalies of total precipitation in the Tau02, Tau04, Tau06, and Tau08 simulations relative to the Tau01 simulation (mm d^{-1}). Regions where the anomalies are statistically significant at the 95% confidence level are hatched. Significance level is estimated using a Student's *t* test from a sample of 20 annual means from the control and each of the simulations.

3. Results

3.1. Tropical Climate Responses

The changes discussed here relate to steady state simulations, and hence, modeled changes include contributions from both direct reduction in deep convection and from dynamical feedback that result due to this reduction. Figure 1 shows the total precipitation in the control simulation (Tau01) and the anomaly of total precipitation in the Tau02, Tau04, Tau06, and Tau08 simulations from the control run, respectively.

The tropical precipitation response varies across different regions. An increase in total precipitation is simulated over the tropical western and equatorial Pacific, and over the Southeast Asian regions with the increase of Tau value (Figures 1b–1e), while a reduction of precipitation is simulated over tropical South America near the Amazon region, tropical Africa, western Arabian Sea, and southeastern leg of the South Pacific Convergence Zone (SPCZ). Among the sensitivity simulations, we will focus on the Tau08 simulation for detailed analysis in this study because the maximum change in deep convective precipitation is simulated in Tau08 when compared to the Tau01 simulation. The tropical precipitation results from Tau01 and Tau08 are compared with the Climate Prediction Center Merged Analysis of Precipitation (CMAP) that covers the period from the year 1979 to year 2000 [*Xie and Arkin*, 1997] (Text S3 and Figure S1 in the supporting information). It is seen that some of the precipitation biases in western Arabian Sea, Arabian Peninsula, southern leg of SPCZ, and Africa are improved in the Tau08 simulation. The pattern correlations between the CMAP data and modeled results over the tropics in the Tau01 and Tau08 simulations are 0.82 and 0.83, respectively. The annual mean tropical precipitation is approximately the same (only a minimum of ~1.8% reduction in Tau02 and maximum of ~2.7% reduction for Tau08; cf. Table 1) over the tropics (20°N to 20°S) in all the simulations.

Figure 2a shows that in the default configuration of the model (control and Tau01), deep convective precipitation contributes about 85% of the annual mean total precipitation in the tropics. The shallow convective precipitation is restricted to off the coasts of southeastern Pacific and southeastern Atlantic Oceans

Table 1. The Annual Mean Total Precipitation (Zonal Mean) and Its Three Components in the Tropics (20°N–20°S) for the Tau Series Simulations and Quadrupled CO_2 Simulation (4×CO2_RF), Calculated Over Both the Land and Ocean Points[a]

Experiment	Total Precipitation (mm d^{-1})	Deep Convective Precipitation (mm d^{-1})	Shallow Convective Precipitation (mm d^{-1})	Stratiform Precipitation (mm d^{-1})
Tau01 (control)	4.36 ± 0.37	3.70 ± 0.31	0.14 ± 0.02	0.51 ± 0.10
Tau02	4.28 ± 0.40	3.44 ± 0.26	0.25 ± 0.07	0.58 ± 0.15
Tau04	4.27 ± 0.60	2.56 ± 0.20	0.63 ± 0.18	1.07 ± 0.32
Tau06	4.26 ± 0.68	1.94 ± 0.14	0.88 ± 0.23	1.42 ± 0.40
Tau08	4.24 ± 0.75	1.54 ± 0.11	1.04 ± 0.27	1.65 ± 0.45
4×CO_2_RF	4.18 ± 0.35	3.57 ± 0.29	0.13 ± 0.02	0.48 ± 0.09

[a]The standard deviations are calculated from the 20-year mean of the Tau series simulations and last 10 years of the 4×CO_2_RF simulation.

(Figure 2b), and it contributes only 3% to the tropical mean. Stratiform precipitation contributes about 12% to the total tropical mean precipitation in the control run (Figure 2c), mainly to the precipitation over the eastern parts of southern tropical oceans and over China.

The contribution of deep convective precipitation to the total annual precipitation in the tropics is reduced to 36% in the Tau08 simulation (Figure 2d and Table 1). However, the contributions of annual shallow convective precipitation and the stratiform precipitation to the total precipitation in the Tau08 simulation are increased to 25% and 39%, respectively (Figures 2e and 2f), compensating the effect on total precipitation. The regions with reduced total precipitation in the Tau08 simulation (cf. Figure 1e) are in general identified with strong convective precipitation in the control simulation (Figure 2a) and largest reductions in deep convection in the Tau08 simulation (Figure 2d).

Figure 3 shows the annual mean vertical profiles of differences (Tau08 − Tau01) of temperature, net condensation (also, Figure 5 (left)), specific humidity, and δD in ambient water vapor (δD_{vapor}). Deep convection

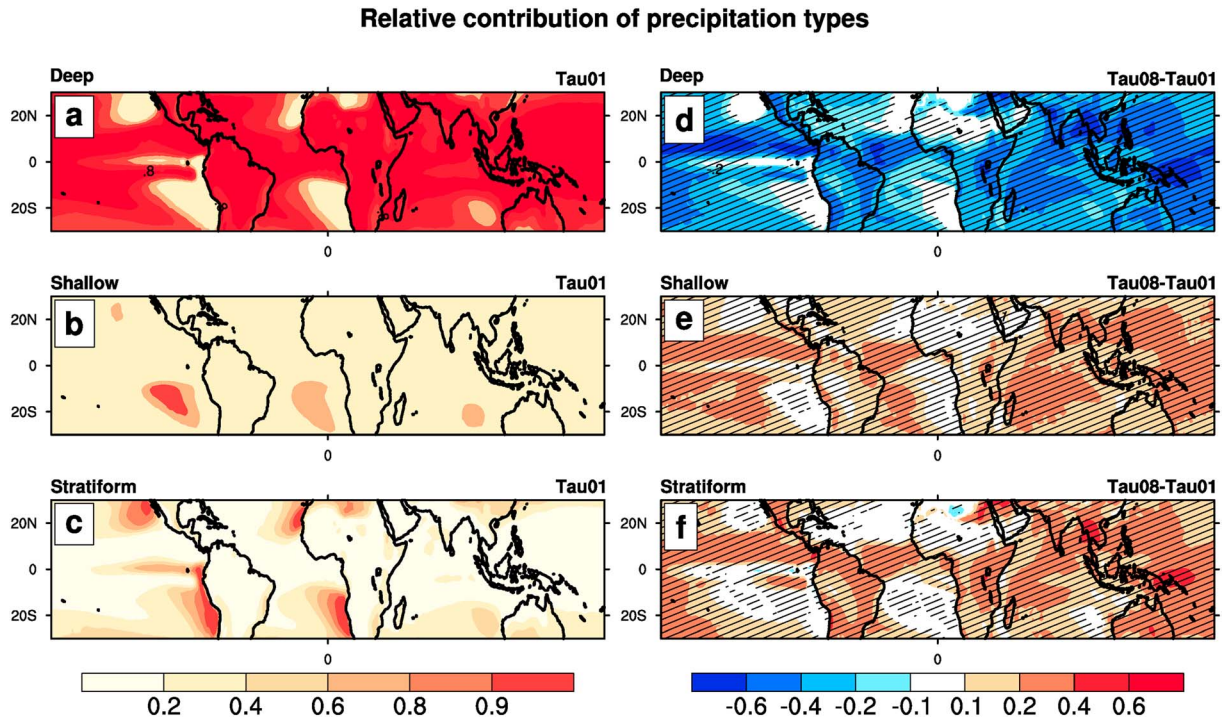

Figure 2. Relative contribution (in fraction) of (a) deep convective precipitation, (b) shallow convective precipitation, and (c) stratiform precipitation to the total precipitation in the Tau01 control simulation and the anomalies of the relative contributions (in fraction) of (d) deep convective precipitation, (e) shallow convective precipitation, and (f) stratiform precipitation in the Tau08 simulation relative to the Tau01 control simulation. Regions where the anomalies are statistically significant at the 95% confidence level are hatched. Significance level is estimated using a Student's *t* test from a sample of 20 annual means from the control and Tau08 simulations.

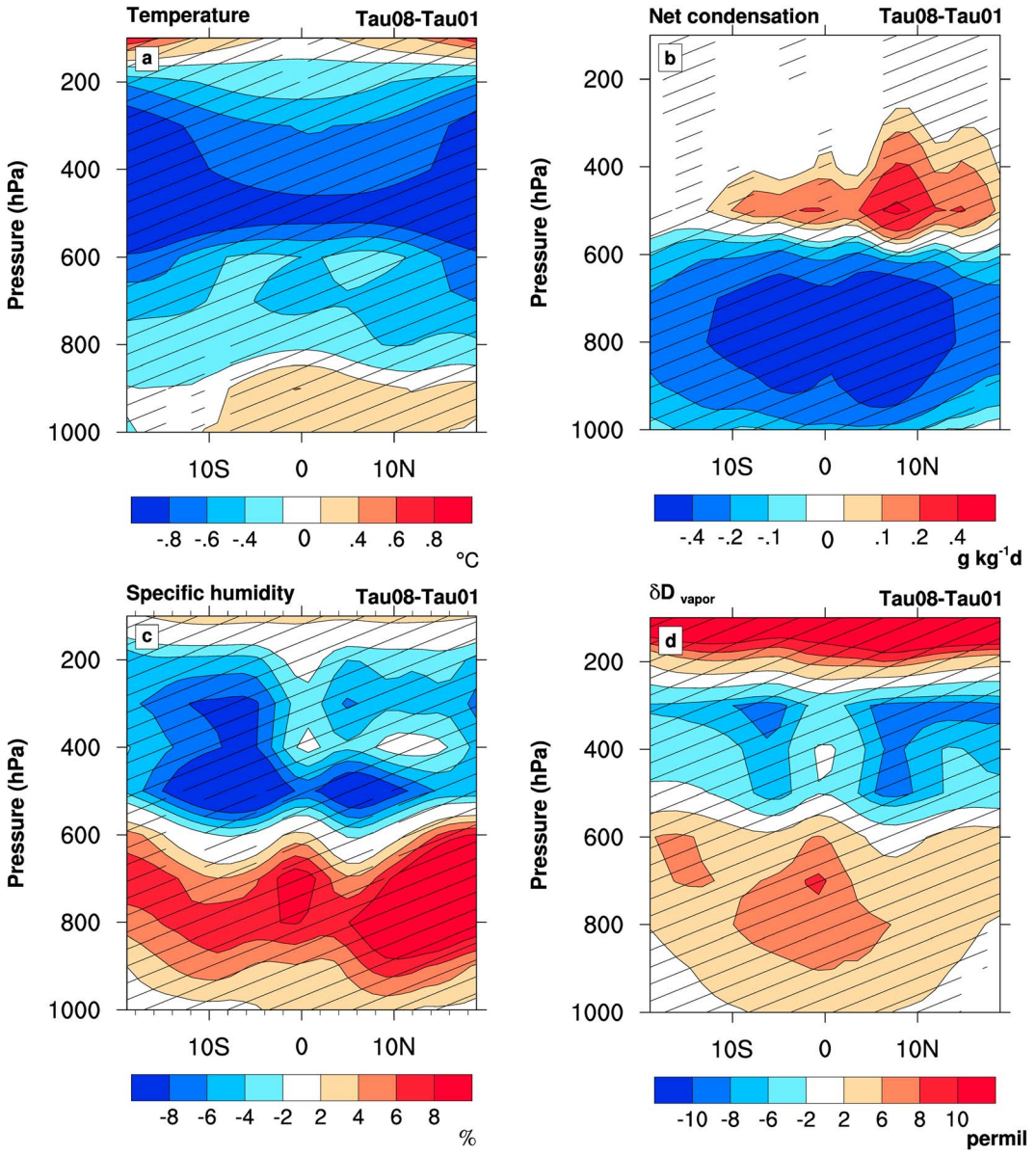

Figure 3. Anomalies of (Tau08 minus Tau01 control simulation) in vertical distributions of zonal mean (a) temperature in °C, (b) net condensation (sum of deep, shallow, and stratiform components; in g/kg/d), (c) specific humidity (percentage change), and (d) δD_{vapor} in (per mil) in the tropics (20°N to 20°S). Regions where the anomalies are statistically significant at the 95% confidence level are hatched. Significance level is estimated using a Student's *t* test from a sample of 20 annual means from the control and Tau08 simulations.

transports the lower level vapor to higher altitudes in the troposphere, so a reduction in the updrafts and condensation through deep convection in the whole atmospheric column in Tau08 simulation causes accumulation of water vapor (q) in the lower levels (Figure 3c) and a reduction of q in the levels between 700 hPa and 150 hPa. Results also show a decrease in the temperature by 0.4°C to 0.8°C between 850 hPa and 250 hPa (Figure 3a) because of reduced deep convection, while a slight increase (+0.4°C) is simulated near the surface because of increased shallow convection.

The annual mean net condensation in the midtroposphere in the Tau08 simulation increases through the shallow convection scheme with a maximum condensation in the 600 hPa level and by the stratiform scheme with a maximum condensation in the 500 hPa level (Figures 3b and 5 (left)). A reduction in the deep convection leads to decreased net condensation in the levels below 600 hPa in the steady state (Figures 3b and 5

(left)), which includes dynamical responses to the reduced deep convection. The changes in mean water vapor (Figure 3c) are consistent with changes in temperature (Figure 3a) in the levels 500 hPa and above, showing that an increase in water vapor in steady state is associated with an increase in temperature and vice versa.

To identify the immediate effect of reduced deep convection before the dynamical responses become substantial, evaluations of the changes in temperature tendency (following *Seager et al*. [2003] and *Wu et al*. [2012]; Figure S2 and Text S4) and net condensation (Figure S3) are done on day 2 for the Tau08 simulation, relative to that of Tau01, using the daily model output. It shows that the troposphere up to 200 hPa level cooled in response to the reduced diabatic heating (sum of heating due to moisture processes, longwave/shortwave radiative processes, and vertical/horizontal diffusion processes) in the Tau08 simulation, and during the first 2 days, the net condensation in the whole troposphere is reduced (Figure S3) due to the suppression of deep convection.

3.2. Isotopic Responses in Atmospheric Water Vapor and Precipitation

As described by the Rayleigh distillation model of water isotope ratios with altitude (successive condensation and consequent depletion of vapor of heavier isotopes as the air parcel ascends), the annual mean δD in ambient water vapor (δD_{vapor}) of the control run decreases with height (Figure S4). In comparison with the control run, positive annual mean δD_{vapor} anomalies (by 2‰–5‰; Figure 3d), in accordance with the reduced net condensation and increased annual mean specific humidity (Figures 3b and 3c, respectively), are simulated in the lower troposphere in the Tau08 simulation. The increased net condensation through shallow convection and stratiform schemes (Figures 3b and 5 (left)) in the midtroposphere causes significantly lower δD_{vapor} values (by 1‰–5‰) between 600 hPa and 300 hPa levels (Figure 3d).

A significant increase of annual mean δD_{vapor} values (8‰–20‰) in the atmospheric levels 250 hPa and above is simulated in the Tau08 simulation (Figure 3d). The anomalies (Tau08 − Tau01) of δD_{vapor} estimated on day 2 also show positive anomalies (Figure S5) in these levels, which are due to the large reduction in net condensation in the whole troposphere due to the reduced deep convection (Figure S3) and hence the reduced upward transport into levels above 250 hPa. Increases in temperature and humidity in the mean statistics (Figures 3a and 3c) above 250 hPa also contribute to these positive anomalies.

Corresponding to the reduction in temperature and net condensation in the day 2 anomalies (Tau08 minus Tau01), a predominant reduction of the reevaporation of precipitation by 20% to 50% in most part of the troposphere, except near surface between the equator and 10°N (Figure S6a), is estimated from the day 2 anomalies. This may also contribute to the higher values of δD_{vapor} in the day 2 anomalies (cf. Figure S5), as, in principle, the reevaporation of relatively depleted condensate can cause lower δD values in the ambient vapor. In the steady state (Figure S6b), condensate reevaporation is reduced by 10% to 50% in the levels between 850 hPa and 200 hPa in the Tau08 simulation along with the reduction in temperature. The steady state reevaporation increases by ~50% in the near surface and upper troposphere above 200 hPa, likely due to the increase in temperature in these levels as discussed in section 3.1. There are other factors in nature that influence the rate of reevaporation, i.e., the effective droplet radius size, and the relative humidity of the ambient atmosphere. However, a significant change in the effective droplet size is absent in the near surface between the Tau08 and Tau01 simulations (Figure S6c). In addition, increased steady state near-surface humidity in Tau08 (cf. Figure 3c) can potentially reduce the reevaporation. Considering these, in our results, we suggest that the other factors are not dominant contributors to the increased steady state reevaporation in the near-surface levels as the increased temperature.

The responses in the condensation rates and δD_{vapor} values to the increases in the τ value in our results agree with the results of *Lee et al*. [2009]. It should be noted that their study used CAM2.0 model, with the value of τ set as 2 h in the control experiment, whereas in our study with IsoCAM3.0, the τ value is set as 1 h in the control experiment.

The annual mean δD values in precipitation (δD_{precip}) anomalies of the Tau02, Tau04, Tau06, and Tau08 simulations from the Tau01 simulation show a gradual transition to higher values of δD_{precip} with increase in τ in the tropics (Figure 4). As indicated earlier, henceforth, we mostly analyze the Tau08 simulation with the strongest response in δD_{precip} among the sensitivity experiments, with Tau01 as the reference simulation. In the tropics, except for western Pacific, δD_{precip} is uniformly enriched in the Tau08 when compared to the

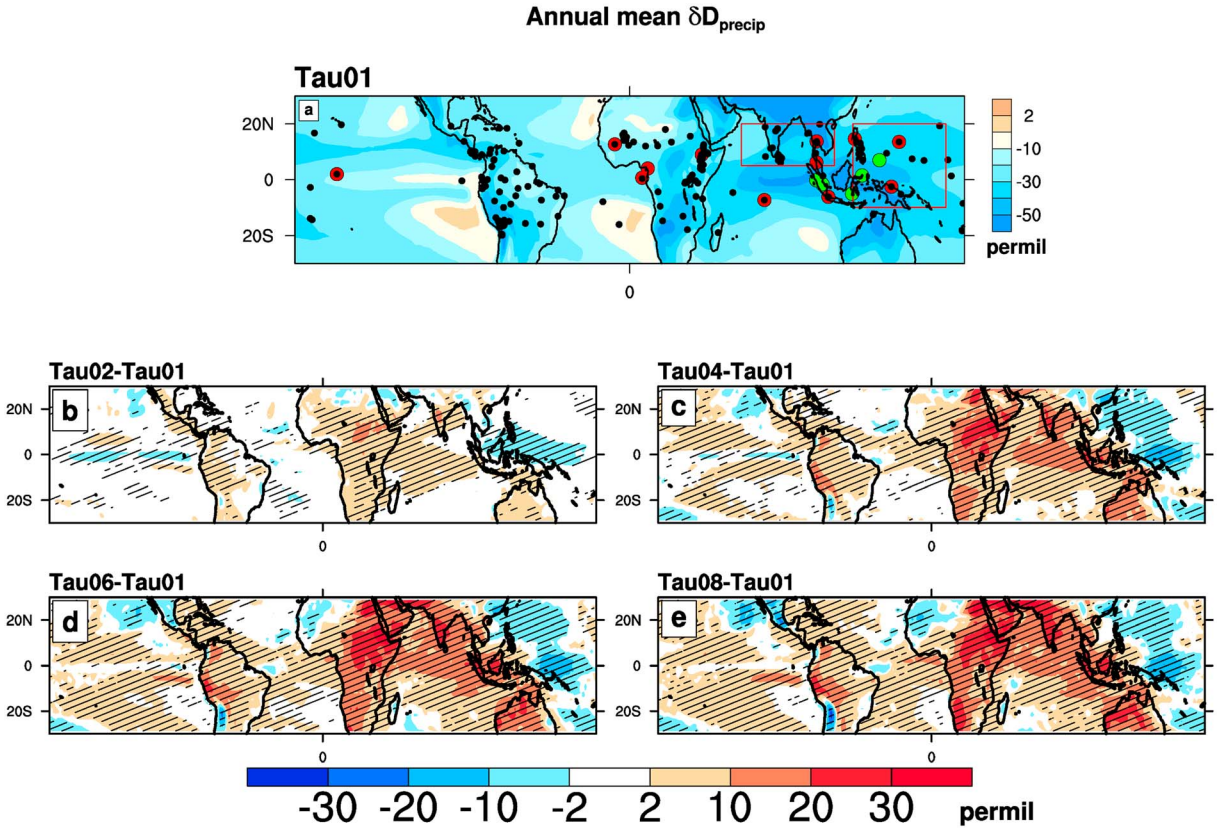

Figure 4. (a) Absolute annual mean values of δD_{precip} in per mil of the control (Tau01) simulation. The black dots represent the GNIP stations in the tropics. The GNIP and JAMSTEC stations selected for the comparison of the site-specific amount effect between the model and observations are shown in red and green dots, respectively. Two boxes overlaid represent SE Asia and western Pacific warm pool regions. (b–e) The anomalies of annual mean δD_{precip} in per mil of the four simulations (Tau02, Tau04, Tau06, and Tau08) in the tropics, relative to the control run. Regions where the anomalies are statistically significant at the 95% confidence level are hatched. Significance level is estimated using a Student's *t* test from a sample of 20 annual mean differences of each of the simulations from the control run.

Tau01 simulation. This is despite an increase in the annual total precipitation simulated in many parts of the tropics (cf. Figure 1e) caused by an increase in the shallow/stratiform precipitation. In particular, over the peninsular India and equatorial eastern Pacific the δD_{precip} values are more positive compared to that of the control, irrespective of an increase in precipitation. This shows that over these regions the effect of reduced deep convection prevails over the effect of increase in total precipitation on the δD_{precip}.

The analysis of the anomalies (Tau08 − Tau01) of the δD composition of convective (sum of deep and shallow precipitation) and stratiform precipitation (Figure S7) shows that the convective precipitation anomalies are enriched with heavier isotopes over the tropics (Figure S7, top), while the stratiform precipitation anomalies are mostly depleted in comparison, except in the central and eastern Africa, equatorial Indian Ocean, and Indian subcontinent (Figure S7, bottom). The seasonal mean (June-July-August-September (JJAS) and December-January-February (DJF)) δD_{precip} anomalies (Figure S8) show qualitatively similar responses as that of the annual means, and it is seen that the respective summer (wet season) anomalies over the land are stronger than that of the winter season.

Figure 5 shows the vertical anomaly (Tau08 − Tau01) profiles of annual mean δD_{vapor}, δD values in the deep convective updrafts ($\delta D_{updraft}$), and in the liquid condensate (δD_{liq}) in the tropics (20°N to 20°S, 180°W to 180°E; Figure 5, left) and the western Pacific warm pool (WPWP; 10°S to 20°N, 120°E to 170°E; Figure 5, right), along with the anomalies of condensation rates from the three precipitation schemes. Absolute values of net condensation for the Tau01 and Tau08 simulations are also shown in this figure. A lack of major difference in the altitude of net condensation between Tau01 and Tau08 simulations in the tropics implies that the effect of reduced net condensation in the lower troposphere is greater on the enrichment of lower level vapor than due to any changes in altitude of condensation. The δD_{vapor} anomalies are comparable to the

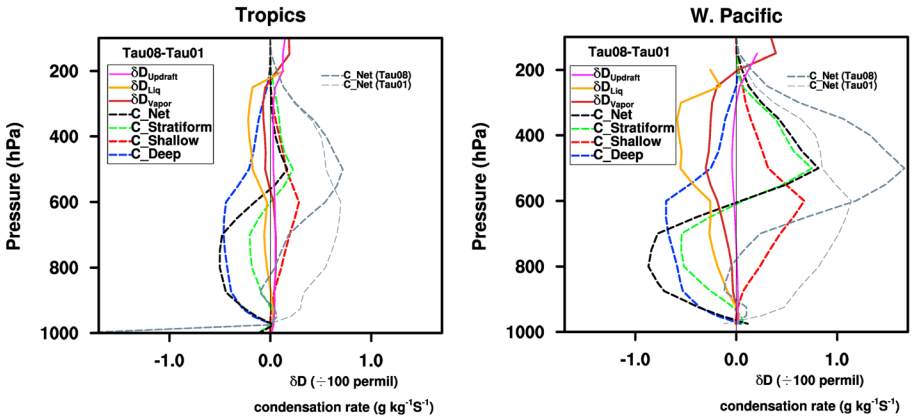

Figure 5. (left) Vertical profile of anomalies (Tau08 minus Tau01) of δD (in per mil; solid color lines in the figures, and the anomalies are scaled by 0.01‰ for plotting) in deep convective updrafts ($\delta D_{updraft}$), condensate (δD_{liq}), and water vapor (δD_{vapor}) in the tropics (20°S–20°N, 180°E–180°W), along with the anomalies in the condensation rates (in dashed color lines) from the deep convective (C_Deep), shallow convective (C_Shallow), and stratiform (C_Stratiform) schemes and net condensation rate (C_Net) (all in g kg^{-1} s^{-1}) of Tau08 simulation relative to the Tau01 control simulation. The gray-colored curves denote the absolute net condensation rate for the Tau01 [C_Net (Tau01)] and Tau08 [C_Net (Tau08)] simulations. (right) Same as in the left plot but in the western Pacific (10°S–20°N, 120°E–170°E).

$\delta D_{updraft}$ anomalies till 600 hPa, likely due to the reduced net condensation and fractionation in the lower troposphere; also, the anomalies of δD_{liq} are positive in the lower troposphere.

In contrast to other tropical oceanic regions, anomalous negative δD_{precip} values are seen in the WPWP (cf. Figure 4), with an increase of total precipitation in the Tau08 simulation. The region differs markedly from the mean tropics in the magnitude of response of the net condensation and δD_{vapor} values in the middle to upper troposphere. Net condensation increases substantially in the 600 hPa to 350 hPa levels (Figure 5, right), and δD_{vapor} and δD_{liq} values in these tropospheric levels are depleted when compared to the whole tropics. It should be noted that in the Tau08 simulation, most of the net condensation in the WPWP happens in middle to upper troposphere and is stronger compared to the whole tropics. Consequently, when compared to a Rayleigh distillation model, the condensate that formed at a higher altitude is more depleted in heavier isotopes (as seen in the δD_{liq} anomalies in Figure 5, right). Additionally, in contrast to the whole tropics, lower tropospheric δD_{vapor} anomalies for this region are negative compared to the control run, despite reduced net condensation in the level. A twofold increase of the pressure velocity at 500 hPa (ω_{500}, <-90 hPa/d; Figure S10) over the region points to vigorous ascending motions triggered by the increased net condensation/latent heat release due to shallow/stratiform condensation associated with the enhanced moisture convergence that leads to increased precipitation. A strong positive feedback between the increased net condensation in the midtroposphere and dynamics in turn causes lowered δD_{vapor} values in the atmospheric column through increased fractionation in the midtroposphere and recycling of the depleted vapor to the lower troposphere. This causes a more isotopically depleted precipitation over the western Pacific compared to the other regions in the tropics.

3.3. Amount Effect

3.3.1. Changes in Amount Effect in Tau Series Experiments

A linear regression analysis between the δD_{precip} values and total precipitation at each model grid point in the tropics is performed to quantify the relationship between the two variables, and the results are shown in Figure 6 and Table 2. The regression coefficient (slope) represents the rate of change of δD_{precip} with unit precipitation amount, while r^2 represents the coefficient of determination that indicates the proportion of variance in δD_{precip} that can be explained by the precipitation amount and varies from 0 to 1 (Table 2). The analysis shows an inverse relationship between the variables (amount effect), which is dominant over the ocean grid points (Figure 6, left). In addition, the maps of both the spatial slopes of amount effect and the spatial correlation coefficients between the annual means of δD_{precip} and total precipitation for the Tau01 and Tau08 simulations are shown in Figure S9. The amount effect in the model is robust and is seen

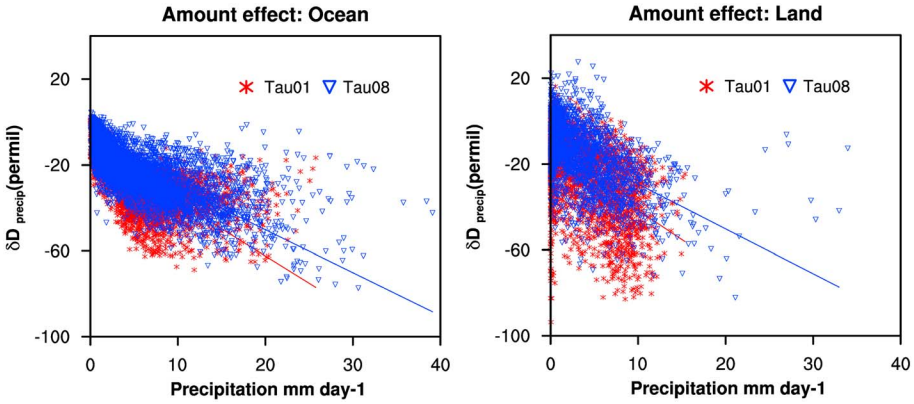

Figure 6. The relationship between climatological monthly mean δD_{precip} values in per mil and total precipitation in mm d^{-1} over (left) tropical ocean and (right) tropical land for Tau01 and Tau08 simulations.

in long-term monthly means (Figure 6 and Table 2), climatological annual means (Figure S9), and mean seasonal data (JJAS and DJF; cf. Table 2), over the tropical ocean for the control simulation, and it is stronger in the monthly means. By definition, the regression slope between climatological monthly means of δD_{precip} values and total precipitation is termed as temporal slope, while the regression slope between climatological annual or seasonal means of δD_{precip} values and total precipitation is termed as spatial slope. Following *Dansgaard* [1964], we focus on the climatological monthly means of δD_{precip} values and total precipitation in the tropics (the temporal slope) to estimate the changes in the slope of regression between the variables in the following discussion.

It should be noted that for the control simulation, the slope of the regression analysis between the climatological monthly mean δD_{precip} values and deep convective precipitation (−2.96‰/mm/d, $r^2 = 0.56$) over the tropical ocean is slightly greater than the regression slope between climatological monthly mean δD_{precip} values and the total precipitation (−2.52‰/mm/d, $r^2 = 0.54$; Table 2). The slope of the amount effect from the climatological monthly mean data over the oceanic grid points in the tropics shows a systematic decrease with increasing τ values (Figure 6 (left) and Table 2). The slope of the relationship from the climatological monthly mean data over the ocean points is reduced to −1.94‰/mm/d ($r^2 = 0.54$) for the Tau08 simulation (reduction by ~23%), which indicates a reduced fractionation efficiency caused by decreased deep convective precipitation. Similarly, the magnitude of the regression slope between the climatological monthly mean δD_{precip} values and total precipitation over the tropical land (Figure 6, right) reduces with increasing Tau, and the value for the control simulation is −2.72‰/mm/d ($r^2 = 0.26$), which is reduced by ~24% to −2.08‰/mm/d ($r^2 = 0.28$) in the Tau08 simulation.

In addition, a reduction in the magnitude of the spatial slope of amount effect is simulated in both the climatological annual and seasonal means (mainly in the JJAS season; Table 2) in the tropical ocean points. The spatial slope of the regression between DJF means of δD_{precip} values and total precipitation in the Tau08 simulation is stronger and has a higher r^2 compared to the JJAS season. This is due to the relatively weaker changes in precipitation and δD_{precip} values in the DJF season compared to the JJAS season, and also due

Table 2. The Slope of the Linear Regression Relation Between the δD_{precip} Values and Total Precipitation Over Oceanic Grid Points for Climatological Monthly and Climatological Seasonal Means in the Simulations and Coefficient of Determination (r^2)

	Climatological Monthly Means		Climatological Seasonal Means			
Experiment	Slope (‰/mm/d)	r^2	DJF Slope (‰/mm/d)	r^2	JJAS Slope (‰/mm/d)	r^2
Tau01	−2.52	0.54	−2.28	0.58	−2.67	0.52
Tau02	−2.46	0.52	−2.31	0.60	−2.60	0.52
Tau04	−2.11	0.52	−2.03	0.65	−2.22	0.51
Tau06	−1.98	0.53	−2.05	0.68	−1.99	0.49
Tau08	−1.94	0.54	−2.08	0.69	−1.91	0.50

Table 3. The Slope of the Linear Regression Between the δD_{precip} Values and Total Precipitation for the Observed Station Data (From the GNIP and JAMSTEC Stations) and Model Simulations for the Tau01 and Tau08 Simulations[a]

				IsoCAM (Long-Term Monthly Means)			
		GNIP (Long-Term Monthly Means)		Tau01		Tau08	
Stations		Slope (‰/mm/d)	r^2	Slope (‰/mm/d)	r^2	Slope (‰/mm/d)	r^2
SE Asia	Diliman (14.64°N, 121°E)	**−1.90**	**0.95**	**−6.46**	**0.84**	**−1.27**	**0.74**
	Diego Garcia (7.31°N, 72.42°E)	**−2.22**	**0.58**	−0.99	0.09	**−2.29**	**0.87**
	Bangkok (13.73°N, 100.5°E)	**−4.02**	**0.79**	**−6.39**	**0.80**	**−1.14**	**0.58**
	Alor Star (6.2°N, 100.40°E)	−1.43	0.39	−2.40	0.18	**−1.78**	**0.71**
WPWP	Taguac Guam (13.55°N, 144.83°E)	**−4.38**	**0.83**	**−4.75**	**0.74**	**−2.08**	**0.84**
	Makasar (5.07°S, 119.55°E)	**−1.57**	**0.68**	**−4.12**	**0.65**	**−1.87**	**0.59**
	Palau (7°N, 134.27°E)	**−3.43**	**0.58**	−0.18	0.01	−1.51	0.32
	Jayapura (2.53°S, 140.72°E)	**−1.78**	**0.55**	1.14	0.2	**−1.89**	**0.76**
	Manado (1.53°N, 124.92°E)	0.66	0.10	−0.94	0.12	**−2.64**	**0.78**
Others	Bamako (12.69°N, 7.99°W)	**−7.76**	**0.9**	−0.19	0.00	−1.81	0.06
	Jambi (1.63°S, 103.65°E)	−2.47	0.18	−7.03	0.34	−1.36	0.49
	Kototabang (0.20°S, 100.32°E)	−1.36	0.20	−1.07	0.04	−1.30	0.25
	Douala-Hydrac (4.03°N, 9.73°E)	−0.77	0.33	**−6.27**	**0.79**	**−3.25**	**0.81**
	Sao Tome (0.68°N, 6.72°E)	**−6.05**	**0.76**	**−4.53**	**0.60**	−2.36	0.42
	Jakarta (6.18°S, 106.83°E)	**−1.29**	**0.56**	**−4.28**	**0.60**	**−1.28**	**0.50**
	Christmas Island (1.98°N, 157.46°W)	**−2.28**	**0.50**	**−1.96**	**0.61**	**−1.63**	**0.61**
	Adis Ababa (9°N, 38.73°E)	−1.81	0.23	−4.47	0.29	−2.02	0.08

[a]The numbers in bold denote the values with r^2 above 0.5.

to the enhanced depletion of δD_{precip} in southern leg of SPCZ during the DJF season, indicating relatively increased fractionation efficiency in the DJF season.

3.3.2. Regional Amount Effect and Comparison With Observations

In order to compare the modeled amount effect with observations, 12 GNIP [*IAEA/GNIP*, 2015] stations in the tropics with at least 3 years of continuous isotope record in precipitation are selected, along with the data from five maritime continent stations in the Asia-Pacific region, collected by the Institute of Observational Research for Global Change (IORGC)/Japan Agency for Marine-Earth Science and Technology (JAMSTEC) [*Kurita et al.*, 2009]. The geographical locations of the stations are shown in Figure 4a. Amount effect from the GNIP and IORGC-JAMSTEC data is estimated from the long-term monthly mean precipitation data and precipitation-weighted δD_{precip} data from these stations (Table 3 and Figure S11). Corresponding amount effect from the model is estimated from the long-term precipitation-weighted monthly mean data averaged over the geographical location of the stations from the Tau01 and Tau08 simulations.

The precipitation-weighted means of δD_{precip} are calculated as

$$\delta_{weighted} = \frac{\sum_{i=1}^{n} P_i \delta_i}{\sum_{i=1}^{n} P_i}$$

where P_i and δ_i are the monthly values of total precipitation and δD_{precip}.

A clear amount effect is seen in the observations from a range of maritime stations in the tropics (cf. Table 3 and Figure S11). The modeled site-specific amount effect from the control run is consistent with the GNIP/IORCG-JAMSTEC data over most of these stations, some with steeper slopes than that of the observations (Table 3). This shows that the model could simulate the isotope variability over the tropics reasonably well. Likewise, we estimate the amount effect for the Tau08 simulation for these stations, and the site-specific slopes of the relationship are, in general, reduced in magnitude compared to the control simulation, irrespective of the changes in total precipitation.

Additionally, the long-term precipitation-weighted annual mean δD_{precip} values from all the available GNIP stations from the tropics, Southeast Asian monsoon regions (5°N–20°N, 60°E–110°E) and western Pacific warm pool (10°S–20°N, 120°E–170°E), are plotted against the corresponding model values in Figure 7. We note that the slopes of amount effect (Table 3) and the δD_{precip} values (Figure 7, left) from the Southeast Asian monsoon regions in the Tau08 simulation are in better agreement with the corresponding GNIP data. In the whole tropics, the slopes of regression between the modeled δD_{precip} values and observations are 0.35

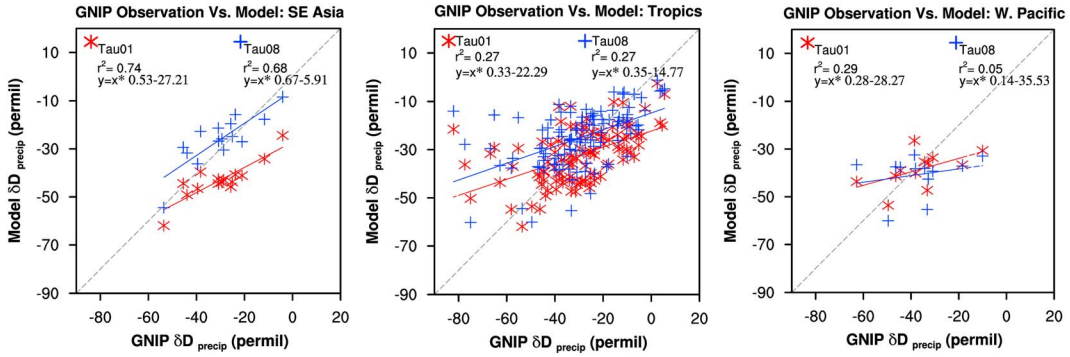

Figure 7. Comparison of absolute values of δD_{precip} in per mil of the GNIP station data (long-term weighted annual mean data from the tropical latitudes) with the corresponding precipitation amount-weighted annual mean grid values from the simulations (Tau01 and Tau08 annual means) in the (left) Southeast Asian monsoon region (5°N–20°N, 60°E–110°E; 15 stations), (middle) whole tropics (20°N–20°S, 180°E–180°W), and the (right) western Pacific (20°N–10°S, 120°E–170°E; 12 stations) region. About 200 stations with valid data in the tropics (20°N–20°S) are selected from the GNIP database, and the names and geographical locations of these stations are available from the GNIP database (accessible at http://www.iaea.org/water). Linear regression statistics for the regions are shown on each plot.

and 0.33, respectively, for the Tau08 and Tau01 simulations (Figure 7, middle), showing a slight improvement in model-data agreement in the Tau08 relative to the control run. The δD_{precip} values in the WPWP region (Figure 7, right) do not show noticeable improvement when compared to the GNIP data in the Tau08 simulation, possibly due to the enhanced depletion of the δD_{precip} values in the region that causes the declining of model-data agreement. However, the site-specific slopes of the amount effect in the Tau08 simulations in a number of stations from the WPWP region are substantially improved when compared to the observations (cf. Table 3). It shows that setting the value of convective relaxation time to 8 h in the Zhang-McFarlane (ZM) convection scheme suggests a method that will lead to improved simulation of isotope ratios in precipitation in the tropics.

3.4. Model Performance With Increase in Tau Values: RMSE Calculations

Root-mean-square error (RMSE) analysis is used to assess the model performance in simulating the δD_{precip} values in the tropics with varying values of Tau. The RMSEs are calculated from the differences between the observations of (i) precipitation-weighted annual means of δD_{precip} and (ii) slope of the site-specific amount effect from the 17 GNIP/JAMSTEC stations in the tropics and corresponding results from the Tau series simulations (cf. section 3.3.2). The data from the additional Tau10 and Tau12 simulations, which are specifically carried out to estimate the RMSEs, are included in the analysis.

The RMSE equation is given by

$$\mathrm{RMSE} = \sqrt{\frac{1}{N}\sum_{i=1}^{N}(\mathrm{Model}_i - \mathrm{Observation}_i)^2}$$

where N (=17) is the number of data samples, $\mathrm{Observation}_i$ is either the long-term weighted monthly δD_{precip} data from the GNIP/JAMSTEC stations or the slope of the amount effect from the stations (cf. Table 3), and Model_i is the corresponding model-simulated value in the observation sites.

Figure 8 shows the RMSEs for both δD_{precip} and slope of amount effect. The RMSEs for the slopes are in the range of 2‰/mm d^{-1} to 3.3‰/mm d^{-1}, whereas the RMSEs of the δD_{precip} are in the range of 8‰ to 13‰. The RMSEs decrease as the Tau values are increased, and the lowest of RMSE values are obtained for the Tau06 and Tau08 simulations for both the parameters. The RMSE values for the slopes and δD_{precip} values reduce by ~32% and ~28%, respectively, for both the Tau06 and Tau08 simulations relative to Tau01. The RMSE values of δD_{precip} increase for Tau values of 10 and 12 h. This shows that overall model performance in simulating the δD_{precip} in the tropics is improved when the Tau values are increased to 6 to 8 h.

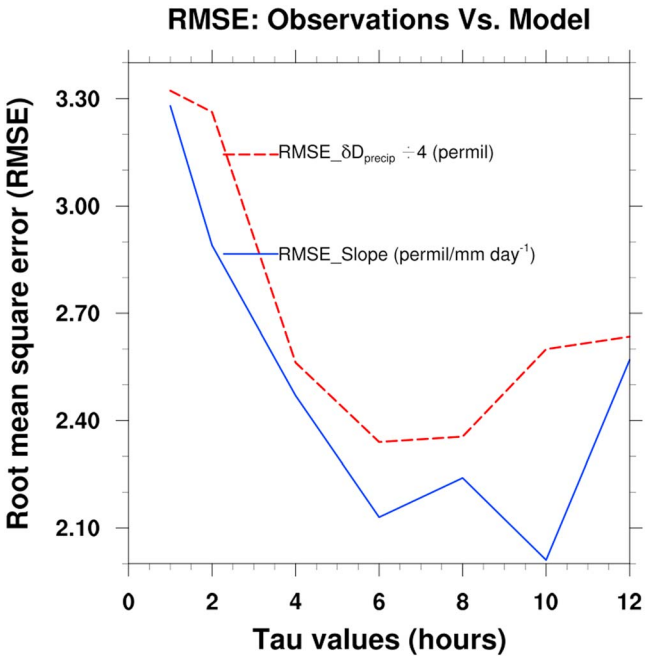

Figure 8. Root-mean-square errors calculated from the differences between (a) the model-simulated precipitation amount-weighted annual means of δD_{precip} in units of per mil and (b) site-specific slope of amount effect calculated from the model results from the Tau series simulations combined with Tau10 and Tau12 simulations over 17 GNIP/JAMSTEC station locations in the tropics and observations from these stations in the units of ‰/mm d^{-1}. The RMSEs for δD_{precip} are scaled by a factor of 0.25‰.

3.5. Changes of Delta Values in the 4×CO_2_RF Experiment

In order to evaluate the impact of enhanced convective activity over land on the amount effect, a quadrupled CO_2 radiative forcing experiment is conducted. Compared to the Tau series experiments, the changes in total precipitation/deep convective precipitation and the isotopic ratios of precipitation in the quadrupled CO_2 radiative forcing experiment are smaller (Figure 9 and Table 1). Unlike the Tau series results, the simulation results show that the percentage contributions of the deep/shallow/stratiform components to total precipitation do not change in the 4×CO_2_RF simulation, so ~85% of the mean annual total precipitation in the tropics is still produced by deep convection (cf. Table 1). The greenhouse gas-induced heating of the land grid cells with respect to the prescribed SST in the 4×CO_2_RF experiment causes an increase of convective activity over the land and reduced convection over the ocean (Figure S12). The contrasting changes in land/ocean precipitation (Figure 9, top) are associated with a global monsoon-type circulation with upward motion over land and downward motion over the ocean (cf. Figure S12) [*Bony et al.*, 2013; *Modak et al.*, 2016]. A warming of 0.3°C to 0.5°C (Figure S13a) caused by the elevated atmospheric CO_2 leads to an increase in specific humidity by 1% to 3% (Figure S13b) in the whole troposphere over the land. The net condensation (Figure S13c) and mean convective precipitation (sum of shallow and deep convective precipitation) are increased over the land, whereas over the ocean the net condensation is decreased and tropical mean deep convective precipitation is reduced by ~6%. Consequently, more negative values of δD_{vapor} (1‰ to 2‰) when compared to the Tau01 are simulated in the middle to lower troposphere over the land points (Figure S13d), whereas slightly more positive values of δD_{vapor} with respect to the control run (up to 1‰) are simulated over the ocean points in these levels. Because of the differential changes in the convection, net condensation, and associated differences in fractionation over the land and the ocean, the δD_{precip} is more positive over the tropical ocean but is more negative over land (Figure 9, bottom).

The changes in the regression slopes between climatological monthly mean δD_{precip} values and the total precipitation over the ocean grid points and land grid points with respect to the control (Tau01) are smaller compared to the Tau series experiments. The slope of the regression between climatological monthly mean δD_{precip} values and the total precipitation over the ocean is −2.70‰/mm/d compared to −2.52‰/mm/d of control run. Because of the increase in convective precipitation, the magnitude of slope of the amount effect from the climatological monthly mean data over land points in the 4×CO_2_RF simulation is slightly increased from 2.78‰/mm/d of the control run to 2.90‰/mm/d.

4. Discussions and Conclusions

Our study shows that the suppression of deep convection in the IsoCAM3.0 model leads to a reduction of net condensation, enrichment of the vapor in the lower troposphere with heavier isotopes, and an enrichment of heavier isotopes in precipitation in the tropics. Correspondingly, with an increase of heavier isotopes in the

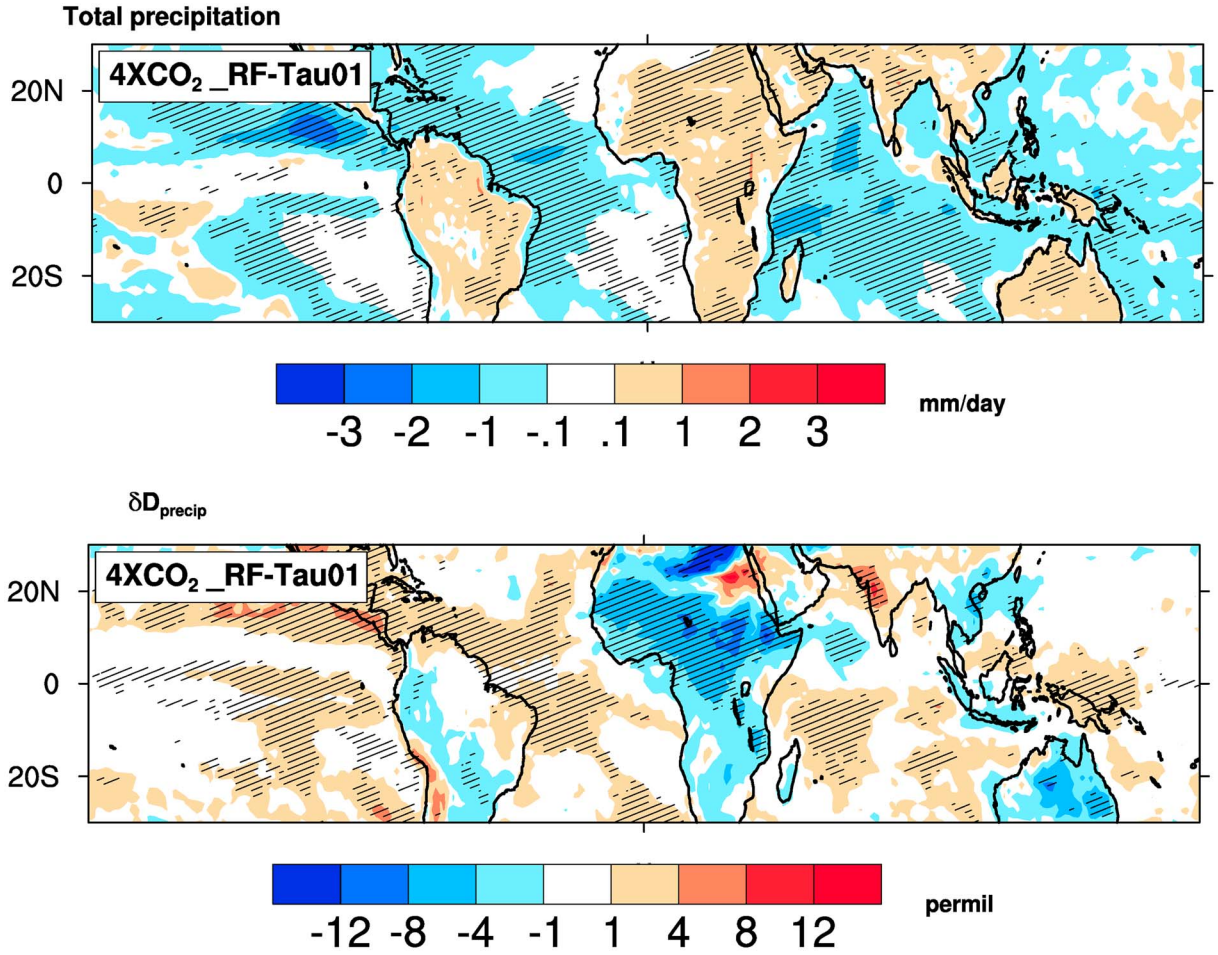

Figure 9. (top) Anomalies of annual mean precipitation in mm d^{-1} in the tropics in the quadrupled CO_2 radiative forcing simulation from the Tau01 control simulation and (bottom) anomalies of δD_{precip} in per mil. Regions where the anomalies are statistically significant at the 95% confidence level are hatched. Significance level is estimated using a Student's *t* test from a sample of 15 annual mean differences of the simulation from the control run.

relatively unchanged mean total precipitation in the tropics, the spatial and temporal slopes of the amount effect reduce. For a reduction of ~60% in mean deep convective precipitation, the magnitude of the regression slope from the long-term monthly means is reduced by ~23% in our simulations. This implies a reduction in the fractionation efficiency associated with weakened deep convection due to a reduction in the lower tropospheric condensation and changes in postcondensation processes such as reduced vapor recycling and increased proportion of condensate reevaporation.

The simulated reduction in deep convective precipitation and the changes in the δD_{vapor} in our simulations in response to the increase in the τ values agree with the results of *Mishra and Srinivasan* [2010] and *Lee et al.* [2009]. Our study is in general agreement with the previous studies [*Jouzel et al.*, 1987; *Schmidt et al.*, 2005; *Lee et al.*, 2009; *Risi et al.*, 2012; *Field et al.*, 2014], which find that the isotope ratios are sensitive to the changes in model parameterizations for cloud and moist processes.

The spatial amount effect in the simulations is seen both over land and predominantly over the ocean, which is noted by the previous modeling studies [*Lee et al.*, 2007; *Risi et al.*, 2008; *Tindall et al.*, 2009] and observations over marine island stations [*Rozanski et al.*, 1993; *Conroy et al.*, 2013]. The difference in the pattern of amount effect over land and ocean is explained by various studies as the effect of advection of replenished vapor to the land from the adjacent oceans and land moisture recycling which dampens the amount effect over the land.

The suppression of deep convection in our Tau series simulations increases the contribution of the shallow convective (formulated by *Hack* [1994] in the model) and stratiform precipitation to the total precipitation in the tropical regions. The midtropospheric depletion of the δD_{vapor} in the Tau08 simulation is due

to the increased net condensation through shallow and stratiform schemes. Furthermore, the suppressed deep convection may reduce the uplifting of enriched vapor from the lower troposphere to middle troposphere [*Sutanto et al*., 2015], leading to more negative δD_{vapor} values in the midtroposphere compared to the control simulation.

It is known that the δD_{precip} is dependent on the isotopic composition of the subcloud layer vapor, and cloud microphysical processes such as degree of condensation and postcondensation processes, i.e., fractionation during reevaporation of rain and equilibration of rain with the surrounding vapor [*Lee and Fung*, 2008; *Risi et al*., 2008; *Conroy et al*., 2013; *Kurita*, 2013]. In our IsoCAM3.0 model, 95% of the stratiform precipitation and 45% of the convective precipitation equilibrate with the lower level vapor, making the precipitation type and also the isotopic composition of lower level vapor and partial equilibration as important factors in the simulated isotopic ratio of precipitation. The steady state tropical annual mean evaporation of precipitation in the near-surface increases in the Tau08 simulation (cf. Figure S6b), which can contribute to the simulated enrichment of isotopes in precipitation [*Wright et al*., 2009] and to a reduced slope of amount effect in the Tau08 simulation. This, in turn, suggests that reduced rain reevaporation during heavy precipitation can be a determinant factor behind the amount effect. In addition, anomalously depleted δD_{vapor} and δD_{precip} over the western Pacific suggest that increased moisture convergence during the strong precipitation events [*Lee et al*., 2007; *Moore et al*., 2014] can be a contributing factor for amount effect along with an increased condensation in the midtroposphere over the region that also implies the effect of increased condensation height on the δD_{precip} values. Despite the reduced net condensation in the lower troposphere over the western Pacific, more negative lower tropospheric δD_{vapor} and δD_{precip} anomalies are simulated in the region, which points to the influence of postcondensation effects including vapor recycling on the δD_{precip} and amount effect. In this study, however, we have not investigated in detail the sensitivity to these postcondensation effects or other microphysical processes on the precipitation isotopes. Instead, we have focused our analysis on the dependence of the isotope amount effect on the deep convective precipitation.

The precipitation isotope ratios in the Southeast Asian monsoon region in the Tau08 simulation are in better agreement with the observations with the improvement in the precipitation in the region (cf. section 3.1). The ratio of deep convective precipitation to the total precipitation in the tropics decreases, and it agrees better with the observations of types of precipitation in the tropics (~43% stratiform fraction over the tropical oceans [*Schumacher and Houze*, 2003]. Furthermore, the model/observations comparison of amount effect over the tropical maritime GNIP/JAMSTEC stations (cf. Table 3) shows that the site-specific slopes of amount effect are improved in the Tau08 simulation, especially in stations from the SE Asia and the WPWP. Our results show that the δD_{precip} in the WPWP is sensitive to the strength of convective activity and relative proportions of the types of precipitation. It is to be noted that in the WPWP, both the precipitation amount (cf. section 3.1) and the precipitation type that changes from ~80% deep convective in the Tau01 to ~50% in the Tau08 simulation are improved when compared to observations (observed values are 50%–70% convective in the western South Pacific [*Yang and Smith*, 2008]).

Our study agrees with *Aggarwal et al*. [2016] that the isotopic ratio of precipitation is sensitive to the proportion of convective/stratiform precipitation. In contrast to our study they find that isotope ratios are negatively correlated with stratiform fractions, while our results show a negative correlation between the isotopic ratio of precipitation and the strength of deep convection. However, the analysis by *Aggarwal et al*. [2016] includes the station data not only from the tropics but also from the subtropics and midlatitudes, where the proportion of stratiform precipitation to the total precipitation is higher; also, the effect of temperature on the isotope ratios is stronger when the tropical and extratropical regions are included in the analysis. Here our analysis is focused only on the tropical region (20°N to 20°S), where the convective rain fraction is higher when compared to the subtropics.

Our study demonstrates the nonstationarity of amount effect at a location with the changes in the precipitation types and convective activity. The proxy-based reconstruction of past precipitation in the tropics is reliant on the spatial or temporal slope of the modern relationship between the precipitation amount and δD_{precip} as the transfer function. The study implies that changes in the convective activity and the relative proportions of precipitation types over a region in the past can shift the slope of past relationship, which can introduce uncertainties in the reconstructed precipitation, so we suggest that caution should be exercised with the reconstruction of past precipitation. Especially, more positive values of isotope ratios in

proxy records may imply a reduction in the deep convection than a reduction in the total precipitation itself. Regionally, we suggest that in the WPWP, proxy records may represent the convective precipitation in the past than the total amount of precipitation, which is in agreement with previous studies [e.g., *Schmidt et al*., 2007; *Kurita et al*., 2009; *Moerman et al*., 2013]. In addition, the use of a local relationship will be more advantageous over applying a modern universal relationship like in some studies [e.g., *Niedermeyer et al*., 2016] to reconstruct the precipitation, especially in regions where the contributions of the convective and stratiform precipitation to the total precipitation differ considerably from the mean representation over the whole tropics.

The quadrupled CO_2 experiment reaffirms a robust inverse relationship between the isotope ratios in precipitation and convective precipitation amount. The changes in isotopic composition in precipitation in the quadrupled CO_2 radiative forcing experiment are smaller when compared to the Tau series of experiments due to the lack of ocean feedback in the experiment.

It should be noted that our results are from a single modeling study and specifically relies on the performance of a specific convective parameterization scheme. While it is likely that the qualitative results could be robust across models, the quantitative results could depend on the climate model and the convection and cloud microphysical parameterization schemes. Although the deep convection is reduced by ~60%, the slope of the tropical amount effect is reduced only by ~23% due to the increased net condensation through the stratiform and shallow schemes in the midtroposphere and the related changes in the dynamics and postcondensation processes.

The present study focuses on the sensitivity of isotopes in precipitation with changes in the deep convection in the model and does not examine the model-data agreement of the δD_{vapor} values, although comparison of the model-simulated δD_{vapor} with the observations from Tropospheric Emission Spectrometer (TES) [*Worden et al*., 2007] will be desirable. However, *Risi et al*. [2012] find that a number of isotope-enabled climate models including the previous version of our model, CAM2.0 [*Lee et al*., 2007], reproduce the isotope distribution in the lower and middle troposphere considerably well, when compared to satellite observations. We compare the isotope values in precipitation with the available GNIP observations to assess the model-data agreement, and importantly, our result is consistent with *Lee et al*. [2009], who find an improved agreement in δD_{vapor} values with the TES satellite data in the 900 hPa to 750 hPa levels when the convective relaxation time scale is increased to 8 h. We suggest that this is applicable to our results as well.

Considering the smaller RMSEs calculated between the predicted isotope ratios in precipitation in the Tau06 and Tau08 simulations and GNIP observations (cf. section 3.4), we suggest that increasing the Tau values to 6 h or 8 h in the ZM convection scheme might lead to better predictions of precipitation in the tropics.

In summary, the sensitivity experiments show the slope of the amount effect; hence, the fractionation efficiency of isotopes reduces due to the reduction in condensation through the deep convection and associated changes in postcondensation effects with a decrease in deep convective precipitation in the model. The influence of reduced deep convection exceeds the effect of increased shallow convection and stratiform precipitation on the amount effect in most of the tropical regions.

Acknowledgments
This study was funded by a grant from the Department of Science and Technology, Government of India. We acknowledge the Supercomputer Education and Research Center, Indian Institute of Science, Bangalore, India, for providing the supercomputer facilities to carry out the model simulations. We thank J. Srinivasan (Indian Institute of Science, Bangalore, India) for the helpful suggestions on our work. The isotopic version of the NCAR Community Atmosphere model was developed with support from the National Science Foundation Paleoclimate Program (award 1049104). The data sets and modeling results are available upon request to the corresponding author (thejna@caos.iisc.ernet.in).

References*

*References for the supplementary information are included in the reference list.
Aggarwal, P. K., U. Romatschke, L. Araguas-Araguas, D. Belachew, F. J. Longstaffe, P. Berg, C. Schumacher, and A. Funk (2016), Proportions of convective and stratiform precipitation revealed in water isotope ratios, *Nat. Geosci.*, doi:10.1038/ngeo2739.
Bala, G., K. Caldeira, and R. Nemani (2010), Fast versus slow response in climate change: Implications for the global hydrological cycle, *Clim. Dyn.*, *35*, 423–434.
Bony, S., C. Risi, and F. Vimeux (2008), Influence of convective processes on the isotopic composition ($\delta^{18}O$ and δD) of precipitation and water vapor in the tropics: 1. Radiative convective equilibrium and Tropical Ocean–Global Atmosphere–Coupled Ocean Atmosphere Response Experiment (TOGA-COARE) simulations, *J. Geophys. Res.*, *113*, doi:10.1029/2008JD009942.
Bony, S., G. Bellon, D. Klocke, S. Sherwood, S. Fermepin, and S. Denvil (2013), Robust direct effect of carbon dioxide on tropical circulation and regional precipitation, *Nat. Geosci.*, *6*(6), 447–451.
Boville, B. A., P. J. Rasch, J. J. Hack, and J. R. McCaa (2006), Representation of clouds and precipitation processes in the Community Atmosphere Model version 3 (CAM3), *J. Clim.*, *19*, 2184–2198.
Burns, S. J., D. Fleitmann, M. Mudelsee, U. Neff, A. Matter, and A. Mangini (2002), A 780-year annually resolved record of Indian Ocean monsoon precipitation from a speleothem from south Oman, *J. Geophys. Res.*, *107*(D20), 4434, doi:10.1029/2001JD001281.
Cao, L., G. Bala, and K. Caldeira (2012), Climate response to changes in atmospheric carbon dioxide and solar irradiance on the time scale of days to weeks, *Environ. Res. Lett.*, *7* 034015.

Chadwick, R., P. Good, T. Andrews, and G. Martin (2014), Surface warming patterns drive tropical rainfall pattern responses to CO_2 forcing on all timescales, *Geophys. Res. Lett.*, *41*, 610–615, doi:10.1002/2013GL058504.
Ciais, P., and J. Jouzel (1994), Deuterium and oxygen 18 in precipitation: Isotopic model, including mixed cloud processes, *J. Geophys. Res.*, *99*(D8), 16,793–16,803.
Collins, J. A., et al. (2011), Interhemispheric symmetry of the tropical African rainbelt over the past 23,000 years, *Nat. Geosci.*, *4*, 42–45.
Collins, J. A., E. Schefuß, S. Mulitza, M. Prange, M. Werner, T. Tharammal, A. Paul, and G. Wefer (2013), Estimating the hydrogen isotopic composition of past precipitation using leaf-waxes from western Africa, *Quat. Sci. Rev.*, *65*, 88–101.
Collins, W. D., P. J. Rasch, B. A. Boville, J. J. Hack, J. R. McCaa, D. L. Williamson, B. P. Briegleb, C. M. Bitz, S. J. Lin, and M. Zhang (2006), The formulation and atmospheric simulation of the Community Atmosphere Model version 3 (CAM3), *J. Clim.*, *19*, 2144–2161.
Conroy, J. L., K. M. Cobb, and D. Noone (2013), Comparison of precipitation isotope variability across the tropical Pacific in observations and SWING2 model simulations, *J. Geophys. Res. Atmos.*, *118*, 5867–5892, doi:10.1002/jgrd.50412.
Contreras-Rosales, L. A., T. Jennerjahn, T. Tharammal, V. Meyer, A. Lückge, A. Paul, and E. Schefuß (2014), Evolution of the Indian summer monsoon and terrestrial vegetation in the Bengal region during the past 18 ka, *Quat. Sci. Rev.*, *102*, 133–148.
Craig, H., and L. I. Gordon (1965), Deuterium and oxygen 18 variations in the ocean and the marine atmosphere.
Dansgaard, W. (1964), Stable isotopes in precipitation, *Tellus*, *16*(4), 436–468.
Deardorff, J. W. (1977), A parameterization of ground-surface moisture content for use in atmospheric prediction models, *J. Appl. Meteorol.*, *16*(11), 1182–1185.
Dong, B., J. M. Gregory, and R. T. Sutton (2009), Understanding land-sea warming contrast in response to increasing greenhouse gases. Part I: transient adjustment, *J. Clim.*, *22*, 3079–3097.
Dykoski, C. A., R. L. Edwards, H. Cheng, D. Yuan, Y. Cai, M. Zhang, Y. Lin, J. Qing, Z. An, and J. Revenaugh (2005), A high-resolution, absolute-dated Holocene and deglacial Asian monsoon record from Dongge Cave, China, *Earth Planet. Sci. Lett.*, *233*, 71–86.
Field, R. D., D. Kim, A. N. LeGrande, J. Worden, M. Kelley, and G. A. Schmidt (2014), Evaluating climate model performance in the tropics with retrievals of water isotopic composition from Aura TES, *Geophys. Res. Lett.*, *41*, 6030–6036, doi:10.1002/2014GL060572.
Gates, W. L., et al. (1999), An overview of the results of the Atmospheric Model Intercomparison Project (AMIP I), *Bull. Am. Meteorol. Soc.*, *80*(1), 29–55.
Gedzelman, S. D., and R. Arnold (1994), Modeling the isotopic composition of precipitation, *J. Geophys. Res.*, *99*(D5), 10,455–10,471, doi:10.1029/93JD03518.
Hack, J. J. (1994), Parameterization of moist convection in the National Center for Atmospheric Research community climate model (CCM2), *J. Geophys. Res.*, *99*(D3), 5551–5568, doi:10.1029/93JD03478.
Hack, J. J., J. M. Caron, S. G. Yeager, K. W. Oleson, M. M. Holland, J. E. Truesdale, and P. J. Rasch (2006), Simulation of the global hydrological cycle in the CCSM Community Atmosphere Model version 3 (CAM3): Mean features, *J. Clim.*, *19*, 2199–2221.
Hoffmann, G., M. Werner, and M. Heimann (1998), Water isotope module of the ECHAM atmospheric general circulation model: A study on timescales from days to several years, *J. Geophys. Res.*, *103*(D14), 16,871–16,896, doi:10.1029/98JD00423.
Hurrell, J. W., J. J. Hack, D. Shea, J. M. Caron, and J. Rosinski (2008), A new sea surface temperature and sea ice boundary dataset for the Community Atmosphere Model, *J. Clim.*, *21*, 5145–5153.
IAEA/GNIP, 2015. Water isotope system for data analysis, visualization, and electronic retrieval. *WISER Version 0.7*. [Available at https://nucleus.iaea.org/wiser on October 2015.]
Jackson, C., M. K. Sen, and P. L. Stoffa (2004), An efficient stochastic Bayesian approach to optimal parameter and uncertainty estimation for climate model predictions, *J. Clim.*, *17*, 2828–2841.
Johnsen, S. J., W. Dansgaard, H. B. Clausen, and C. C. Langway (1972), Oxygen isotope profiles through the Antarctic and Greenland ice sheets, *Nature*, *235*(5339), 429–434.
Jouzel, J., G. L. Russell, R. J. Suozzo, R. D. Koster, J. W. C. White, and W. S. Broecker (1987), Simulations of the HDO and $H_2{}^{18}O$ atmospheric cycles using the NASA GISS general circulation model: The seasonal cycle for present-day conditions, *J. Geophys. Res.*, *92*(D12), 14,739–14,760.
Kurita, N. (2013), Water isotopic variability in response to mesoscale convective system over the tropical ocean, *J. Geophys. Res. Atmos.*, *118*, 10,376–10,390, doi:10.1002/jgrd.50754.
Kurita, N., K. Ichiyanagi, J. Matsumoto, M. D. Yamanaka, and T. Ohata (2009), The relationship between the isotopic content of precipitation and the precipitation amount in tropical regions, *J. Geochem. Explor.*, *102*, 113–122.
Laskar, A. H., M. G. Yadava, R. Ramesh, V. J. Polyak, and Y. Asmerom (2013), A 4 kyr stalagmite oxygen isotopic record of the past Indian summer monsoon in the Andaman Islands, *Geochem. Geophys. Geosyst.*, *14*, 3555–3566, doi:10.1002/ggge.20203.
Lawrence, J. R., S. D. Gedzelman, D. Dexheimer, H. K. Cho, G. D. Carrie, R. Gasparini, C. R. Anderson, K. P. Bowman, and M. I. Biggerstaff (2004), Stable isotopic composition of water vapor in the tropics, *J. Geophys. Res.*, *109*, doi:10.1029/2003JD004046.
Lee, J. E., and I. Fung (2008), "Amount effect" of water isotopes and quantitative analysis of post condensation processes, *Hydrol. Process.*, *22*, 1–8, doi:10.1002/hyp.6637.
Lee, J. E., I. Fung, D. J. DePaolo, and C. C. Henning (2007), Analysis of the global distribution of water isotopes using the NCAR atmospheric general circulation model, *J. Geophys. Res.*, *112*, doi:10.1029/2006JD007657.
Lee, J. E., R. Pierrehumbert, A. Swann, and B. R. Lintner (2009), Sensitivity of stable water isotopic values to convective parameterization schemes, *Geophys. Res. Lett.*, *36*, doi:10.1029/2009GL040880.
Lekshmy, P. R., M. Midhun, R. Ramesh, and R. A. Jani (2014), ^{18}O depletion in monsoon rain relates to large scale organized convection rather than the amount of rainfall, *Sci. Rep.*, *4*, doi:10.1038/srep05661.
Lorius, C., C. Ritz, J. Jouzel, L. Merlivat, and N. Barkov (1985), A 150,000-year climatic record from Antarctic ice, *Nature*, *316*, 591–596.
Majoube, M. (1971), Fractionnement en oxygene-18 et en deuterium entre l'eau et sa vapeur, *J. Chim. Phys.*, *68*(10), 1423–1436.
Manabe, S. (1969), Climate and the ocean circulation 1: The atmospheric circulation and the hydrology of the Earth's surface, *Mon. Weather Rev.*, *97*(11), 739–774.
Managave, S. R., M. S. Sheshshayee, R. Ramesh, H. P. Borgaonkar, S. K. Shah, and A. Bhattacharyya (2011), Response of cellulose oxygen isotope values of teak trees in differing monsoon environments to monsoon rainfall, *Dendrochronologia*, *29*, 89–97.
Merlivat, L., and G. Nief (1967), Fractionnement isotopique lors des changements d 'état solide-vapeur et liquide-vapeur de l'eau à des températures inférieures à 0°C, *Tellus*, *19*(1), 122–127.
Mishra, S. K., and J. Srinivasan (2010), Sensitivity of the simulated precipitation to changes in convective relaxation time scale, *Ann. Geophys.*, *28*(10), 1827–1846.
Modak, A., G. Bala, L. Cao, and K. Caldeira (2016), Why must a solar forcing be larger than a CO_2 forcing to cause the same global mean surface temperature change?, *Environ. Res. Lett.*, *11*(4), 044013, doi:10.1088/1748-9326/11/4/044013.

Moerman, J. W., K. M. Cobb, J. F. Adkins, H. Sodemann, B. Clark, and A. A. Tuen (2013), Diurnal to interannual rainfall δ^{18}O variations in northern Borneo driven by regional hydrology, *Earth Planet. Sci. Lett.*, *369*, 108–119.

Moore, M., Z. Kuang, and P. N. Blossey (2014), A moisture budget perspective of the amount effect, *Geophys. Res. Lett.*, *41*, 1329–1335, doi:10.1002/2013GL058302.

Niedermeyer, E. M., M. Forrest, B. Beckmann, A. L. Sessions, A. Mulch, and E. Schefuß (2016), The stable hydrogen isotopic composition of sedimentary plant waxes as quantitative proxy for rainfall in the West African Sahel, *Geochim. Cosmochim. Acta*, *184*, 55–70.

Noone, D. (2003), June. Water isotopes in CCSM for studying water cycles in the climate system, in *8th Annual CCSM workshop*, Breckenridge, Colorado.

Noone, D., and C. Sturm (2010), Comprehensive dynamical models of global and regional water isotope distributions, in *Isoscapes: Understanding Movement, Pattern, and Process on Earth Through Isotope Mapping*, pp. 195–219, Springer Verlag.

Noone, D., and I. Simmonds (2002), Associations between δ^{18}O of water and climate parameters in a simulation of atmospheric circulation for 1979–95, *J. Clim.*, *15*(22), 3150–3169.

Pausata, F. S., D. S. Battisti, K. H. Nisancioglu, and C. M. Bitz (2011), Chinese stalagmite [delta] 18O controlled by changes in the Indian monsoon during a simulated Heinrich event, *Nat. Geosci.*, *4*, 474–480.

Risi, C., S. Bony, and F. Vimeux (2008), Influence of convective processes on the isotopic composition (δ^{18}O and δD) of precipitation and water vapor in the tropics: 2. Physical interpretation of the amount effect, *J. Geophys. Res.*, *113*, doi:10.1029/2008JD009943.

Risi, C., S. Bony, F. Vimeux, C. Frankenberg, D. Noone, and J. Worden (2010a), Understanding the Sahelian water budget through the isotopic composition of water vapor and precipitation, *J. Geophys. Res.*, *115*, doi:10.1029/2010JD014690.

Risi, C., S. Bony, F. Vimeux, and J. Jouzel (2010b), Water stable isotopes in the LMDZ4 general circulation model: Model evaluation for present day and past climates and applications to climatic interpretations of tropical isotopic records, *J. Geophys. Res.*, *115*, doi:10.1029/2009JD013255.

Risi, C., et al. (2012), Process evaluation of tropospheric humidity simulated by general circulation models using water vapor isotopologues: 1. Comparison between models and observations, *J. Geophys. Res.*, *117*, doi:10.1029/2011JD016621.

Rozanski, K., L. Araguás-Araguás, and R. Gonfiantini (1993), Isotopic patterns in modern global precipitation, *Climate change in continental isotopic records*, 1–36.

Sano, M., R. Ramesh, M. S. Sheshshayee, and R. Sukumar (2011), Increasing aridity over the past 223 years in the Nepal Himalaya inferred from a tree-ring δ^{18}O chronology, *The Holocene*, doi:10.1177/0959683611430338.

Schefuß, E., S. Schouten, and R. R. Schneider (2005), Climatic controls on central African hydrology during the past 20,000 years, *Nature*, *437*(7061), 1003–1006.

Schefuß, E., H. Kuhlmann, G. Mollenhauer, M. Prange, and J. Pätzold (2011), Forcing of wet phases in southeast Africa over the past 17,000 years, *Nature*, *480*, 509–512.

Schmidt, G. A., G. Hoffmann, D. T. Shindell, and Y. Hu (2005), Modeling atmospheric stable water isotopes and the potential for constraining cloud processes and stratosphere-troposphere water exchange, *J. Geophys. Res.*, *110*, doi:10.1029/2005JD005790.

Schmidt, G. A., A. N. LeGrande, and G. Hoffmann (2007), Water isotope expressions of intrinsic and forced variability in a coupled ocean-atmosphere model, *J. Geophys. Res.*, *112*, doi:10.1029/2006JD007781.

Schumacher, C., and R. A. Houze Jr. (2003), Stratiform rain in the tropics as seen by the TRMM precipitation radar, *J. Clim.*, *16*(11), 1739–1756.

Scinocca, J. F., and N. A. McFarlane (2004), The variability of modeled tropical precipitation, *J. Atmos. Sci.*, *61*, 1993–2015.

Seager, R., N. Harnik, Y. Kushnir, W. Robinson, and J. Miller (2003), Mechanisms of hemispherically symmetric climate variability, *J. Clim.*, *16*(18), 2960–2978.

Stenni, B., et al. (2004), A late-glacial high-resolution site and source temperature record derived from the EPICA Dome C isotope records (East Antarctica), *Earth Planet. Sci. Lett.*, *217*(1), 183–195.

Sturm, C., Q. Zhang, and D. Noone (2010), An introduction to stable water isotopes in climate models: Benefits of forward proxy modeling for paleoclimatology, *Climate of the Past*, *6*, 115–129.

Sutanto, S. J., G. Hoffmann, R. A. Scheepmaker, J. Worden, S. Houweling, K. Yoshimura, I. Aben, and T. Röckmann (2015), Global-scale remote sensing of water isotopologues in the troposphere: Representation of first-order isotope effects, *Atmos. Meas. Tech.*, *8*(3), 999–1019.

Tharammal, T., A. Paul, U. Merkel, and D. Noone (2013), Influence of Last Glacial Maximum boundary conditions on the global water isotope distribution in an atmospheric general circulation model, *Climate of the Past*, *9*(2), 789–809.

Tierney, J. E., S. C. Lewis, B. I. Cook, A. N. LeGrande, and G. A. Schmidt (2011), Model, proxy and isotopic perspectives on the East African humid period, *Earth Planet. Sci. Lett.*, *307*, 103–112.

Tindall, J. C., P. J. Valdes, and L. C. Sime (2009), Stable water isotopes in HadCM3: Isotopic signature of El Niño–Southern Oscillation and the tropical amount effect, *J. Geophys. Res.*, *114*, doi:10.1029/2008JD010825.

Vuille, M., R. S. Bradley, M. Werner, R. Healy, and F. Keimig (2003), Modeling δ^{18}O in precipitation over the tropical Americas: 1. Interannual variability and climatic controls, *J. Geophys. Res.*, *108*(D6), doi:10.1029/2001JD002038.

Vuille, M., M. Werner, R. S. Bradley, and F. Keimig (2005), Stable isotopes in precipitation in the Asian monsoon region, *J. Geophys. Res.*, *110*, doi:10.1029/2005JD006022.

Williamson, D. L. (2013), The effect of time steps and time scales on parameterization suites, *Q. J. R. Meteorol. Soc.*, *139*(671), 548–560, doi:10.1002/qj.1992.

Williamson, D. L., and J. G. Olson (1994), Climate simulations with a semi-Lagrangian version of the NCAR community climate model, *Mon. Weather Rev.*, *122*(7), 1594–1610.

Williamson, D. L., and P. J. Rasch (1994), Water vapor transport in the NCAR CCM2, *Tellus A*, *46*(1), 34–51.

Worden, J., et al. (2007), Importance of rain evaporation and continental convection in the tropical water cycle, *Nature*, *445*, 528–532.

Wright, J. S., A. H. Sobel, and G. A. Schmidt (2009), Influence of condensate evaporation on water vapor and its stable isotopes in a GCM, *Geophys. Res. Lett.*, *36*, doi:10.1029/2009GL038091.

Wu, Y., R. Seager, M. Ting, N. Naik, and T. A. Shaw (2012), Atmospheric circulation response to an instantaneous doubling of carbon dioxide. Part I: Model experiments and transient thermal response in the troposphere, *J. Clim.*, *25*, 2862–2879.

Xie, P., and P. A. Arkin (1997), Global precipitation: A 17-year monthly analysis based on gauge observations, satellite estimates, and numerical model outputs, *Bull. Am. Meteorol. Soc.*, *78*(11), 2539.

Yadava, M. G., and R. Ramesh (2005), Monsoon reconstruction from radiocarbon dated tropical Indian speleothems, *The Holocene*, *15*, 48–59.

Yadava, M. G., R. Ramesh, and G. B. Pant (2004), Past monsoon rainfall variations in peninsular India recorded in a 331-year-old speleothem, *The Holocene*, *14*, 517–524.

Yang, S., and E. A. Smith (2008), Convective-stratiform precipitation variability at seasonal scale from 8 yr of TRMM observations: Implications for multiple modes of diurnal variability, *J. Clim.*, *21*(16), 4087–4114.

Yang, B., Qian, Y., Lin, G., Leung, L.R., Rasch, P.J., Zhang, G.J., McFarlane, S.A., Zhao, C., Zhang, Y., Wang, H. and Wang, M., 2013. Uncertainty quantification and parameter tuning in the CAM5 Zhang-McFarlane convection scheme and impact of improved convection on the global circulation and climate. *J. Geophys. Res. Atmos.*, *118*, 395–415, doi:10.1029/2012JD018213.

Zhang, G. J., and N. A. McFarlane (1995), Sensitivity of climate simulations to the parameterization of cumulus convection in the Canadian Climate Centre general circulation model, *Atmos. Ocean*, *33*(3), 407–446.